Experimental Study on Backward Wave Oscillators Using Dielectric Discharge Cold Cathodes*)

Masamichi SAKAGAMI, Akira SUGAWARA, Takeru OTSUKI, Yuta ANNAKA, Min Thu SAN, Kiyoyuki YAMBE, Kazuo OGURA and Wonsop KIM[1)]

Graduate School of Science and Technology, Niigata University, Niigata 950-2181, Japan
[1)]*Department of New & Renewable Energy Electrical Engineering, Jeonnam Provincial College, Korea*

(Received 21 December 2017 / Accepted 7 August 2018)

Herein, we investigated the characteristics of a backward wave oscillator using a dielectric discharge cold cathode (DDCC) in a weakly relativistic region with energies less than 100 keV. The DDCC comprises a copper disc electrode and a ceramic tube; the DDCC exhibited a circular burn pattern with a voltage less than about 30 kV. When a Marx generator was used as a high-voltage source, two microwave oscillations (first phase and second phase) were observed. Within 80 periods of the slow-wave structure, we observed microwave oscillation at the π-point with a voltage of about 30 kV and then detected a microwave signal of about 910 - 5500 mW.

Keywords: electron beam, cold cathode, microwave generation, weakly relativistic region, backward wave oscillator, π-point operation

DOI: 10.1585/pfr.13.3406107

1. Introduction

Recently, high-power microwave sources with small sizes and variable frequencies are desired for plasma heating in nuclear fusion processes, radars, communication systems, measuring systems, and medical equipment. One such microwave source is the backward wave oscillator (BWO) [1–5]. A cold cathode, used inside the BWO, does not need to be heated by a power supply, thereby enabling miniaturization. To this end, the cold cathode must produce high current and a fairly uniform annular electron beam in a weakly relativistic region, less than 100 kV.

For high-power microwave generation, π-point operation is important [6,7]. The group velocity near the π-point is low, and the interaction between the electron beam and a corrugated slow-wave structure (SWS) is strong. The generated microwave is not only amplified but also absorbed by the SWS, as the π-point exists at the upper cutoff frequency of the SWS. Therefore, the microwaves are observed only for few special cases. The π-point operation of the SWS occurs when a short-period SWS (20 periods) is used. D. Li *et al.* [6] and Min Thu San *et al.* [7] demonstrated this phenomenon both theoretically and experimentally, respectively. In this study, the occurrence of microwave oscillations at the π-point, i.e., the operation of the BWO around 30 keV is investigated. Our aim is to develop compact and vehicle-movable THz-microwave sources. Thus, investigating certain conditions of the π-point operation is important.

In this study, a dielectric discharge cold cathode (DDCC), comprising an alumina ceramic tube and a copper disk, is used [8]. An electron beam is emitted from a triple junction of copper, ceramic, and vacuum. The DDCC is applied to a W-band BWO (75 - 110 GHz). The annular shape electron beam moves through the SWS (80 periods) in an axial magnetic field of $B_z = 0.819$ T. The beam voltage is approximately 30 kV for the π-point operation.

Min Thu San *et al.* [9] investigated the relationship between power and SWS length. Specifically, they detected microwave powers of about 1000 mW and about 150 mW at the π-point, for 40 and 80 periods, respectively, using a velvet-wrapped cathode. The power decreased as the length increased, finally disappearing at 120 periods. Using the DDCC, we detected a microwave power of about 5500 mW for 80 periods of the same SWS at the π-point.

This paper is organized as follows. Section 2 describes electron beam and microwave generation using the BWO device. Section 3 discusses the experimental results, i.e., the properties of the DDCC, beam current, and microwave generation, especially π-point operation. Finally, Section 4 concludes the paper.

2. Experimental Set-Up

2.1 Dielectric Discharge Cold Cathode (DDCC)

The emitted electron beam should interact effectively with the slow wave excited near the surface of the SWS to oscillate the microwave as a BWO. For a high-power microwave to oscillate in a weakly relativistic region of around 30 kV, generating a fairly uniform electron beam

author's e-mail: akira@eng.niigata-u.ac.jp

*) This article is based on the presentation at the 26th International Toki Conference (ITC26).

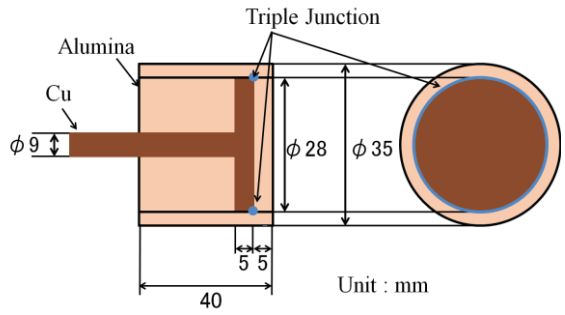

Fig. 1 DDCC schematic.

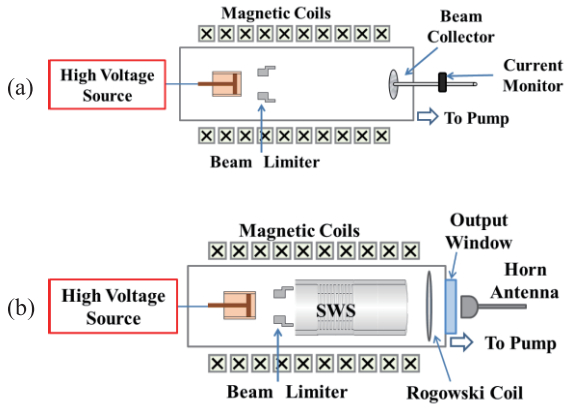

Fig. 2 Schematic diagram of the BWO device: (a) burn pattern experiment and (b) the microwave oscillation experiment.

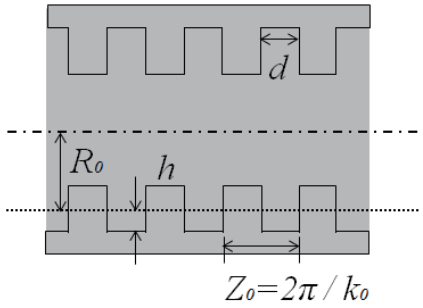

Fig. 3 Schematic diagram of the W-band SWS.

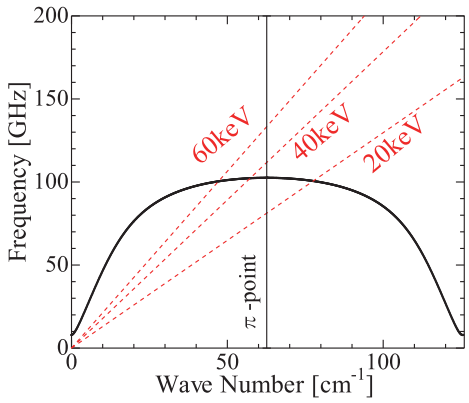

Fig. 4 Dispersion curve of the SWS and beam lines.

with an annular shape is necessary.

Figure 1 shows the size of the DDCC. The DDCC has a constant distance of 5 mm from the triple junction to the ceramic cylinder edge. When high voltage is applied to the DDCC, the electric field concentrates at the triple junction. Next, electrons are emitted first via field emission and then through the creeping discharge from the ceramic cylinder edge.

2.2 Backward Wave Oscillator (BWO)

Figure 2 shows the schematic diagram of the BWO device. Figure 2 (a) shows the set-up for the burn pattern experiment. The burn pattern is observed using a thermally sensitive paper placed on a beam collector. Figure 2 (b) shows the set-up for the microwave oscillation experiment.

In this study, we used a W-band SWS (75 - 110 GHz). The beam current was measured using a Rogowski coil installed in the BWO device, and the emitted microwave was observed via a horn antenna of F-band (90 - 140 GHz), installed outside the output window, with a cutoff frequency of 74 GHz.

The BWO comprises the DDCC, a high voltage source, a 29.7-mm-diameter beam limiter (anode), a W-band SWS, a vacuum system, and external magnetic field coils.

As the high voltage source, a magnetic pulse compression (MPC: MPC3010S-25LN, Suematsu Denshi Co. Ltd.; output energy: about 0.5 J/pulse; pulse rise time: < 50 ns) in the region of 30 kV or less, or a Marx generator (MG: IG-H200, Nichicon Corporation; total capacitance: 0.05 μF; waveform: 1.2/50 μs) in the region of 30 kV or more was used. The distance between the ceramic cylinder edge and the beam limiter was 10 mm. The pressure in the BWO was maintained below 4×10^{-3} Pa, and an axial magnetic field of 0.819 T was applied.

Figure 3 shows the structure of the W-band SWS. The waveguide is made of aluminum, and its dimensions are as follows: average radius $R_0 = 15.1$ mm, corrugation amplitude $h = 0.30$ mm, corrugation width $d = 0.30$ mm, periodic length $Z_0 = 0.50$ mm, and total length $L = 80 \times Z_0$.

Figure 4 shows the dispersion curve of the SWS. The broken lines are beam lines of 20, 40, and 60 keV, as labeled. A beam energy of about 30 keV works as the π-point operation at the upper cutoff frequency, which is about 100 GHz.

3. Experimental Results and Discussion

3.1 Electron beam generation

Generating a high current density electron beam at low beam energies around 30 keV is necessary to oscillate a high-power microwave. In this section, the electron beam emission characteristics (current–voltage character-

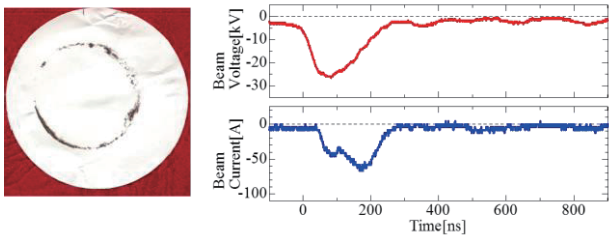

Fig. 5 Burn pattern and waveforms of the DDCC.

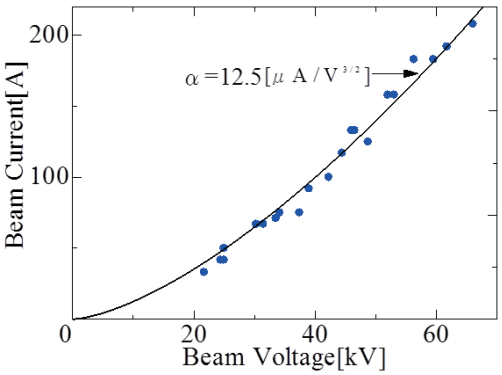

Fig. 6 Beam current-voltage characteristics of the DDCC.

istics and burn pattern) of the DDCC are measured.

Figure 5 shows the burn pattern and the simultaneously obtained waveforms. The burn pattern was observed by 5 shots at about 26 kV using the MPC. The emitted electron beam passed through the beam limiter and reached the beam collector. At this instance, a peak current of 66.7 A was observed at a beam voltage of 26.0 kV.

As the outside diameter of the burn pattern is approximately 28 mm, it is considered to be determined by the inside diameter of the ceramic cylinder. The thickness of the electron beam is about 1.5 mm.

Figure 6 shows the current–voltage characteristics of the DDCC. When high voltage is applied to the DDCC, an electron beam is emitted from the ceramic cylinder edge and is measured by a current monitor connected to the beam collector. The beam voltage is observed via a high-voltage probe. The beam current increases with the beam voltage, and was observed to be about 67.0 A at 30 kV. The curve in the figure follows Child–Langmuir's law and is expressed by the following equation:

$$\text{Electron Beam Current} = \alpha V^{3/2}, \quad (1)$$

where α is the proportional constant, and V [V] is the beam voltage. Figure 6 depicts a curve calculated using (1) with $\alpha = 12.5\,[\mu\text{A/V}^{3/2}]$. The property of the DDCC fits the Child–Langmuir's law well. Thus, the electron beam current is limited by the space charge.

3.2 Microwave generation

Figure 7 shows the waveforms of the beam voltage, beam current, and detected microwave signal, when the

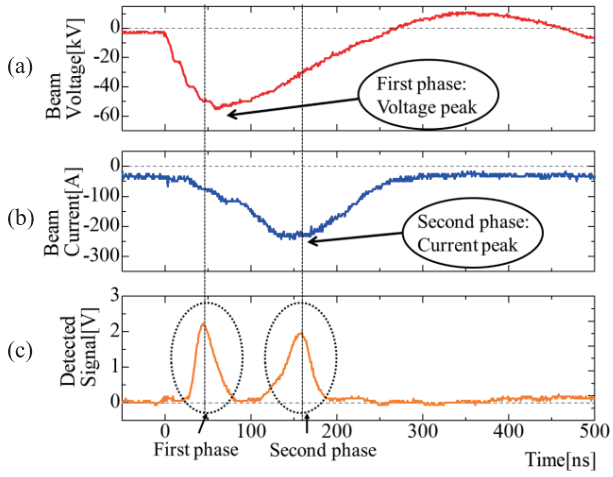

Fig. 7 Typical waveforms: (a) voltage, (b) beam current, and (c) the detected microwave signal.

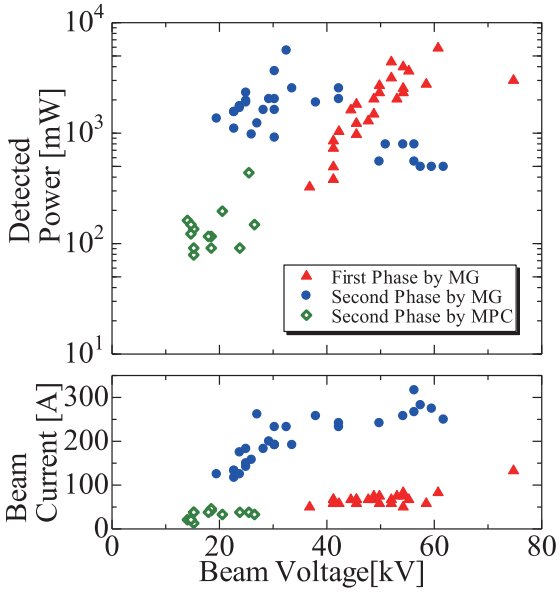

Fig. 8 Detected microwave power and beam current versus beam voltage at the peak timing of the detected microwave signal shown in Fig. 7.

MG was used as the high-voltage source. When an MG with a large capacitor was used, two microwave signals were observed. The first microwave peak (first phase) was observed near the voltage peak timing, and the second microwave peak (second phase) was observed near the current peak timing. When the MPC was used, the detected microwave signal was observed only at the second phase.

The beam voltage, beam current, and detected power were plotted at the peak timing of the detected microwave signal in Fig. 8. BWO using the DDCC detected a stable microwave power of about 80 - 160 mW at a low beam voltage of about 15 kV. The maximum power was 5880 mW at a beam voltage of 60.7 kV. In the second phase, the detected microwave power was in the range of

910 - 5500 mW at the π-point. We observed π-point operation for a long 80-period SWS using the DDCC.

π-point operation was not observed using a velvet-wrapped cathode for the first phase, as it was not found in Ref. [9]. On the other hand, microwave oscillations were observed around 30 kV in the second phase when using the DDCC.

In the SWS, the region above 30 kV is a traveling wave region, and the region below 30 kV is a backward wave region. Also, the region around 30 kV is the π-point region. As the group velocity around the π-point region is small, and the interaction between the electron beam and SWS is strong, operation at the π-point is necessary for high-power microwave oscillation in BWOs. Therefore, the microwave is observed in some special cases. One notable point is that the period of the SWS is short 20 periods [7]. Reflection is large at the edge of the SWS; however, the microwave has transverse direction at the edge and hence, leaks from the SWS [7]. A part of the leaked microwave on the cathode side is reflected by the cathode and emitted from the output window. A theoretical study of the overall operation of surface-wave oscillators from BWO to travelling wave tubes (TWT) indicates that radiation is not expected near the π-point or under the Bragg condition [6, 10]. However, Min Thu San *et al.* [7] experimentally confirmed that microwaves are generated in the region of the π-point when a short-period SWS (20 periods) is used. The other notable point is that a large current flows during the second phase. When using the DDCC, the beam current flowed in the second phase, and the microwave was detected. At the π-point, microwave oscillation has a large growth rate but also large damping. The DDCC can emit a stable annular beam at approximately 30 kV near the π-point. Furthermore, the microwaves were generated in the second phase by increasing the beam current to about 100 A or more and maintaining that state for a long duration about 200 ns. K. Hahn *et al.* [11] and K. Yambe *et al.* [12] also observed current peak delay from the voltage peak timing using disk and rectangular cathodes, respectively. It is likely that pulse-shortening rarely occurs in the second phase when using the DDCC [11]. Pulse-shortening limits long-pulse operation (> 100 ns) in high-power Cherenkov devices, but beam current continues to flow in the DDCC for approximately 300 ns with a peak value of approximate 250 A (see Fig. 7). Therefore, in case of long SWSs of 80 periods, it is considered that microwave oscillation was observed on the BWO using the DDCC.

In summary, the following experimental results were obtained. In the first phase, the maximum detected microwave power was 5880 mW with a beam voltage of 60.7 kV. In the second phase, the detected microwave power was in the range of 910 - 5500 mW at the π-point. The oscillation frequency was around 100 GHz. However, analysis of the emission pattern is necessary to identify the microwave output.

4. Conclusions

In this study, electron beam emission characteristics (current–voltage characteristics and burn pattern) and microwave oscillation characteristics were examined in a weakly relativistic region below 100 kV.

The burn pattern exhibited an annular shape. It is considered that the DDCC can generate high density plasma at the triple junction.

As shown in Fig. 8, we observed microwave oscillations in both the BWO and TWT in the first phase, with beam currents less than approximately 100 A. Oscillations at the π-point were observed in the second phase, when the beam currents were larger than approximately 200 A. In the second phase, the detected microwave power was in the range of 910 - 5500 mW at the π-point.

In future work, experiments using a large-capacity power supply, which can sustain high current and long-pulse operations, will be used to clarify the principles underlying the oscillations at the π-point.

[1] A.V. Gunin *et al.*, IEEE Trans. Plasma Sci. **26**, no.3, 326 (1998).
[2] D.K. Abe *et al.*, IEEE Trans. Plasma Sci. **26**, no.3, 2781 (1998).
[3] N. Vlasov *et al.*, IEEE Trans. Plasma Sci. **28**, no.3, 550 (2000).
[4] H. Yoshimura *et al.*, Plasma Fusion Res. **5**, S2093 (2010).
[5] M. Takahashi *et al.*, J. Korean Phys. Soc. **59**, 3573 (2011).
[6] D. Li *et al.*, Appl. Phys. Lett. **100**, 191101 (2012).
[7] M.T. San *et al.*, IEEE Trans. Plasma Sci. **45**, no.1, 30 (2017).
[8] Y. Kido *et al.*, 2015 Pacific Symposium on Pulsed Power and Applications, S1-5 (2015).
Available: http://p3e.ttu.edu/symp2015/images/Technical_Program_2015PSPPA.pdf
[9] M.T. San *et al.*, Plasma Fusion Res. **11**, 2406085 (2016).
[10] H.L. Andrews *et al.*, Phys. Rev. ST Accel. Beams **8**, 050703 (2005).
[11] K. Hahn *et al.*, IEEE Trans. Plasma Sci. **30**, no.3, 1112 (2002).
[12] K. Yambe *et al.*, IEEE Trans. Plasma Sci. **41**, 2781 (2013).